


Article

Tri- and Mono-Nuclear Zinc(II) Complexes Based on Half- and Mono-Salamo Chelating Ligands

Xiu-Yan Dong, Lei Gao, Fei Wang, Yang Zhang and Wen-Kui Dong * 

School of Chemical and Biological Engineering, Lanzhou Jiaotong University, Lanzhou 730070, China; dxy568@163.com (X.-Y.D.); GaoLei19910731@163.com (L.G.); wangfei3986@163.com (F.W.); zhangy8124@163.com (Y.Z.)

* Correspondence: dongwk@126.com; Tel.: +86-931-4938-703

Academic Editor: Sławomir J. Grabowski

Received: 25 July 2017; Accepted: 30 August 2017; Published: 1 September 2017

Abstract: Two newly designed complexes, $[Zn(L^1)(EtOH)]$ (**1**) and $[Zn(L^2)(OAc)_2]_2Zn \cdot CHCl_3$ (**2**) derived from salamo and half-salamo chelating ligands (H_2L^1 and HL^2) have been synthesized and characterized by elemental analyses, IR and UV-VIS spectra, fluorescence spectra, and X-ray crystallography. Complex **1** shows a slightly distorted tetragonal pyramid and forms an infinite 3D supramolecular structure. All of the Zn(II) ions in complex **2** are hexa-coordinated with slightly distorted octahedral geometries. Complex **2** possesses an infinite 2D space structure. The fluorescence titration experiments were used to characterize fluorescence properties of complexes **1** and **2**. And the normalized fluorescent spectra exhibit that complexes **1** and **2** have favourable fluorescent emissions in different solvents.

Keywords: salamo-type ligand; complex; synthesis; crystal structure; fluorescence properties

1. Introduction

As we know, Salen-type ligands ($R-CH=N-(CH_2)_2-N=CH-R$) and their metal complexes have been extensively investigated in modern coordination chemistry for several decades [1–5], which have been extensively investigated in potential application in biological fields [6–13], electrochemical conducts [14,15], nonlinear optical materials [16–20], magnetic materials [21–25], luminescence properties [26–32], and supramolecular architecture [33–37], and so on. Chemical modifications of substituent or functional groups in the Salen N_2O_2 ligands are effective in exchanging the structures or the main functions of complexes, such as salamo ligand, a Salen analogue, ($R-CH=N-O-(CH)_n-O-N=CH-R$) is one of the most versatile ligands and the large electronegativity of oxygen atoms is expected to strongly affect the electronic properties of the N_2O_2 coordination sphere, which can lead to different and novel structures and properties of the resulting complexes [38].

Due to the unique structure of salamo-type complexes, a study shown that it is at least 104 times more stable than salen-type complexes [39]. The Zn(II) ion does not produce spectroscopic or magnetic signals because of its $3d^{10}4s^0$ electronic configuration, when the Zn(II) ion forms complexes with ligands, the complexes generally have fluorescence properties [40,41]. Although these salamo-type Zn(II) complexes are currently being studied and developed, the solvent effects on the salamo-type Zn(II) complexes are still very rare. In order to further study the syntheses, crystal structures and fluorescence properties of the Zn(II) complexes with the salamo-type ligands, herein, two new complexes $[Zn(L^1)(EtOH)]$ (**1**) and $[Zn(L^2)(OAc)_2]_2Zn \cdot CHCl_3$ (**2**) with salamo and half-salamo ligands H_2L^1 and HL^2 have been reported, especially the study of the half-salamo ligand and its complex is reported firstly. Half-salen ligands and their metal complexes have been extensively investigated in modern coordination chemistry for a long time [42,43], but at present, no literature has shown that half-salamo ligands and their metal complexes have been synthesized.

2. Experimental

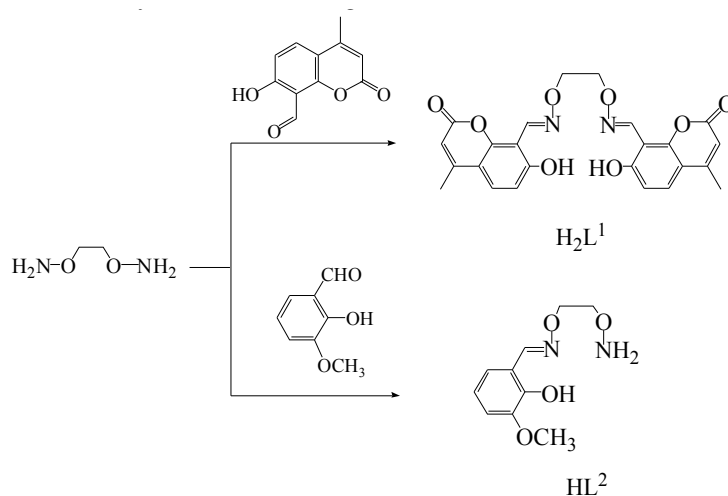
2.1. Materials and Methods

7-Hydroxyl-4-methyl-coumarin and 3-methoxysalicylaldehyde of 98% purity were purchased from Alfa Aesar and used without further purification (New York, NY, USA). The other reagents and solvents were analytical grade reagents from Tianjin Chemical Reagent Factory (Tianjin, China).

C, H and N analyses were obtained using a GmbH VarioEL V3.00 automatic elemental analysis instrument (Berlin, Germany). Elemental analyses for zinc were detected with an IRIS ER/S-WP-1 ICP atomic emission spectrometer (Berlin, Germany). Melting points were obtained by the use of a microscopic melting point apparatus made by Beijing Taike Instrument Company Limited and were uncorrected. IR spectra were recorded on a Vertex70 FT-IR spectrophotometer, with samples prepared as KBr (500–4000 cm^{-1}) and CsI (100–500 cm^{-1}) pellets (Bruker AVANCE, Billerica, MA, USA). UV-VIS absorption spectra were recorded on a Shimadzu UV-3900 spectrometer (Shimadzu, Japan). Luminescence spectra in solution were recorded on a Hitachi F-7000 spectrometer (Shimadzu, Japan). ^1H NMR spectra were determined by a German Bruker AVANCE DRX-400 spectrometer (Bruker AVANCE, Billerica, MA, USA). X-ray single crystal structure determinations were carried out on a Bruker Smart Apex CCD diffractometer (Bruker AVANCE, Billerica, MA, USA).

2.2. Synthesis of H_2L^1

The major reaction steps involved in the synthesis of H_2L^1 and HL^2 are given in Scheme 1. 8-Formyl-7-hydroxy-4-methylcoumarin was prepared according to reported procedure [44]. 1,2-Bis(aminooxy)ethane was synthesized following the literature [45–47].



Scheme 1. Synthetic route to H_2L^1 and HL^2 .

H_2L^1 : A solution of 8-formyl-7-hydroxy-4-methyl-coumarin (768.76 mg, 2.9 mmol) in methanol (25 mL) was added to a solution of 1,2-bis(aminooxy)ethane (92.00 mg, 1.0 mmol) in methanol (25 mL). The suspension solution was stirred and refluxed at 65 °C for 4 h, and then a yellowish solid of the salamo-type ligand (H_2L) was obtained, which was collected by suction filtration. Yield: 83.2%, m.p. 287–288 °C. Anal. Calcd for $\text{C}_{24}\text{H}_{20}\text{N}_2\text{O}_8$ (%): C, 62.07; H, 4.34; N, 6.03. Found: C, 61.84; H, 4.41; N, 6.06. ^1H NMR (400 MHz, CDCl_3), δ 10.72 (s, 2H), 8.95 (s, 2H), 7.50 (d, J = 8.9 Hz, 2H), 6.93 (d, J = 8.9 Hz, 2H), 6.14 (s, 2H), 4.54 (s, 4H), 2.40 (s, 6H).

2.3. Synthesis of HL^2

HL^2 : An methanol solution (25 mL) of 3-methoxysalicylaldehyde (1 mmol, 152.6 mg) was added dropwisely to 1,2-bis(aminooxy)ethane (1.5 mmol, 138.0 mg) in methanol solution (25 mL).

The resulting mixed solution was heated for 3 h between 55 and 60 °C temperature range. The solution was concentrated in vacuo and the residue was purified by column chromatography (SiO₂, chloroform/ethyl acetate, 30:1) to afford a colourless flocculent crystalline solid, then the half-salamo-type ligand (HL²) was obtained, which was collected by suction filtration. Yield: 79.4%. m.p. 91–92 °C. Anal. Calc. for C₁₀H₁₄N₂O₄ (%): C 53.09; H 6.24; N 12.38. Found: C 53.21; H 6.19; N 12.29. ¹H NMR (400 MHz, CDCl₃), δ 9.87 (s, 1H), 8.22 (s, 1H), 6.91 (dd, *J* = 7.9, 1.5 Hz, 1H), 6.86 (s, 1H), 6.80 (dd, *J* = 7.7, 1.7 Hz, 1H), 5.52 (s, 2H), 4.40–4.33 (m, 2H), 4.00–3.94 (m, 2H), 3.91 (s, 3H).

2.4. Synthesis of Complex 1

To a ethanol solution (2 mL) of zinc(II) acetate dehydrate (0.01 mmol, 2.19 mg), and a solution of H₂L¹ (0.01 mmol, 4.64 mg) in 6 mL of dichloromethane was added dropwise, and immediately the mixed solution colour changed to yellow. The mixture solution was filtered and the filtrate was allowed to stand for two weeks. Through partial solvent evaporation, single crystals suitable for X-ray diffraction analysis were obtained after two weeks. Yield: 48.2%. Anal. Calcd for C₂₆H₂₄N₂O₉Zn ([Zn(L¹)(EtOH)] (1)) (%): C, 54.42; H, 4.22; N, 4.88; Zn, 11.39. Found: C, 54.29; H, 4.29; N, 4.80; Zn, 11.25.

2.5. Synthesis of Complex 2

To a methanol solution (1 mL) of zinc(II) acetate dehydrate (0.03 mmol, 6.57 mg), and a solution of HL² (0.02 mmol, 9.28 mg) in 2 mL of chloroform was added dropwise, The colour of the mixing solution turned to yellow immediately, then the mixture was filtered and the filtrate was obtained. The single crystals suitable for X-ray diffraction studies were obtained by vapour diffusion of diethyl ether into the filtrate for two days at room temperature. Yield: 52.6%. Anal. Calcd for C₂₉H₃₉Cl₃N₄O₁₆Zn₃ ([{ZnL²(OAc)₂]₂Zn]·CHCl₃ (2)) (%): C, 34.76; H, 3.92; N, 5.59; Zn, 19.57. Found: C, 34.55; H, 3.98; N, 5.37; Zn, 19.26.

2.6. Crystal Structure Determinations of Complexes 1 and 2

The crystal diffractometer provides a monochromatic beam of Mo Kα radiation (0.71073 Å) produced using Graphite monochromator from a sealed Mo X-ray tube was used for obtaining crystal data for complexes 1 and 2 at 173.00(10) and 292.38(10), respectively. The LP factor semi-empirical absorption corrections were applied using the SADABS program. The structures were solved by the direct methods (SHELXS-2014) [48]. The H atoms were included at the calculated positions and constrained to ride on their parent atoms. All non-hydrogen atoms were refined anisotropically using a full-matrix least-squares procedure on *F*² with SHELXL-2014 [48]. The crystal data and experimental parameters relevant to the structure determinations are listed in Table 1.

Crystallographic data have been deposited with the Cambridge Crystallographic Data Centre as supplementary publication, No. CCDC 1564063 and 1564062 for complexes 1 and 2. Copies of the data can be obtained free of charge on application to CCDC, 12 Union Road, Cambridge CB21EZ, UK (Telephone: (44) 01223 762910; Fax: +44-1223-336033; E-mail: deposit@ccdc.cam.ac.uk). These data can be also obtained free of charge at www.ccdc.cam.ac.uk/conts/retrieving.html.

Table 1. Crystal data and structure refinement parameters for complexes 1 and 2.

Complex	1	2
Formula	C ₂₆ H ₂₄ N ₂ O ₉ Zn	C ₂₉ H ₃₉ Cl ₃ N ₄ O ₁₆ Zn ₃
Formula weight	573.84	1002.16
Temperature (K)	173.00(10)	292.38(10)
Wavelength (Å)	0.71073	0.71073
Crystal system	Monoclinic	Triclinic
Space group	<i>P</i> 2 ₁ / <i>n</i>	<i>P</i> −1

Table 1. Cont.

Complex	1	2
Unit cell dimensions		
<i>a</i> (Å)	12.811(3)	13.1694(13)
<i>b</i> (Å)	13.4725(9)	13.3568(13)
<i>c</i> (Å)	15.393(3)	16.1452(14)
α (°)	90	94.664(8)
β (°)	107.665(19)	113.074(10)
γ (°)	90	112.722(9)
<i>V</i> (Å ³)	2531.6(8)	2317.6(4)
<i>Z</i>	4	2
<i>D_c</i> (g cm ^{−3})	1.506	1.430
μ (mm ^{−1})	1.028	1.775
<i>F</i> (000)	1184	1012
Crystal size (mm)	0.24 × 0.19 × 0.17	0.22 × 0.18 × 0.14
θ Range (°)	3.338–25.008	3.34–26.02
Index ranges	−13 ≤ <i>h</i> ≤ 15, −16 ≤ <i>k</i> ≤ 14, −14 ≤ <i>l</i> ≤ 18	−10 ≤ <i>h</i> ≤ 16, −16 ≤ <i>k</i> ≤ 16, −19 ≤ <i>l</i> ≤ 15
Reflections collected	8334	16,912
Independent reflections	4446	9102
<i>R</i> _{int}	0.0996	0.0522
Completeness	99.6%	99.79%
Data/restraints/parameters	4446/16/349	9102/1/502
GOF	1.001	0.963
Final <i>R</i> ₁ , <i>wR</i> ₂ indices	0.0581/0.0934	0.0633/0.1473
<i>R</i> ₁ , <i>wR</i> ₂ indices (all data)	0.0721/0.1598	0.1236/0.1774
Largest differences	0.926/−0.772	0.873/−0.587
	peak and hole (e Å ^{−3})	

3. Results and Discussion

Complexes **1** and **2** constructed from salamo and half-salamo chelating ligands (H₂L¹ and HL²) have been synthesized, and characterized by IR spectra, UV-VIS spectra, and X-ray crystallography analyses. The fluorescence titration experiments were used to characterize fluorescence properties of complexes **1** and **2**. The normalized fluorescent spectra exhibits that complexes **1** and **2** have favourable fluorescent emissions in different solvents.

3.1. IR Spectra

The FT-IR spectra of H₂L¹ and HL² with their corresponding complexes **1** and **2** exhibit various bands in the 4000–400 cm^{−1} region (Figure 1). A typical C=N stretching band of the free ligands H₂L¹ and HL² appears at 1619 and 1604 cm^{−1}, and that of complexes **1** and **2** at 1581 and 1597 cm^{−1}, respectively [49]. The C=N stretching frequencies are shifted to low frequencies, indicating that the Zn(II) atoms are coordinated by azomethine nitrogen atoms of (L¹)^{2−} and (L²)^{1−} moieties. Therefore, the conclusion could be made that H₂L¹ and HL² coordinated with Zn(II) atoms [50]. The typical C=O stretching band at 1728 cm^{−1} was exhibited by the free ligands H₂L¹, where at 1712 cm^{−1} show the C=O stretching band in complex **1**. The free ligands H₂L¹ and HL² exhibit Ar–O stretching frequencies at 1288 and 1249 cm^{−1}, while the Ar–O stretching frequencies of the complexes **1** and **2** appear at 1226 and 1242 cm^{−1}, respectively. The Ar–O stretching frequencies are shifted to low frequencies, which could be evidence of the Zn–O bond formation between Zn(II) atoms and oxygen atoms of phenolic groups [51].

The far-IR spectra (550–100 cm^{−1}) of both complexes **1** and **2** were also obtained so as to identify the bonds of Zn–O and Zn–N frequencies. The bands at 447 and 463 cm^{−1} of complexes **1** and **2** can be attributed to $\nu_{(\text{Zn-O})}$, while the bands at 516 and 564 cm^{−1} are assigned to $\nu_{(\text{Zn-N})}$ [52].

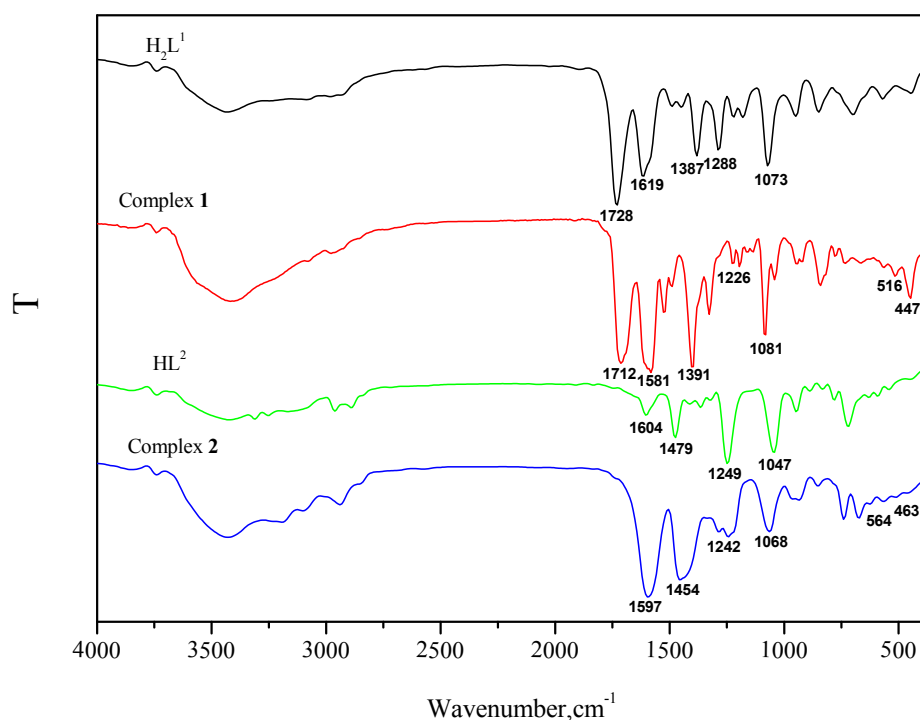


Figure 1. The FT-IR spectra of the ligands and their complexes **1** and **2** (cm^{-1}).

3.2. Crystal Structure of Complex 1

As depicted in Figure 2 and Table 2, complex **1** crystallizes in the monoclinic space group $P2_1/n$, which consists of one Zn(II) ion, one completely deprotonated $(L^1)^{2-}$ unit, and one coordinated ethanol molecule. The Zn(II) ion is penta-coordinated by two oxime nitrogen (N1 and N2) atoms and two phenoxo oxygen (O3 and O6) atoms, the four atoms are all from one deprotonated $(L^1)^{2-}$ unit, and one oxygen (O9) atom from the coordinated ethanol molecule (Figure 2a). The coordination environment around the Zn(II) ion is best described as a slightly distorted trigonal bipyramidal geometry, which obtains the geometry adopted by the Zn(II) ion, and the τ value was estimated to be $\tau = 0.845$ (Figure 2b) [53,54]. The phenolic oxygen (O3) and the oxime nitrogen (N2) of the $(L^1)^{2-}$ unit and one oxygen (O9) atom of the coordinated ethanol molecule constitute, together, the basal plane (Zn1–O3, 1.940(5) Å; Zn1–N2, 2.036(7) Å and Zn1–O9, 2.049(6) Å), and other phenolic oxygen (O6) and oxime nitrogen (N1) atoms of the $(L^1)^{2-}$ unit occupy the axial positions (Zn1–O6, 1.994(5) and Zn1–N1, 2.187(7) Å). The three coordination atoms on the base plane and the Zn(II) ion is 0.062(3) Å displaced from the mean plane [55,56]. Additionally, four of the intramolecular C10–H10...O2, C11–H11A...O9, C13–H13...O7, and C25–H25B...O6 hydrogen bonds were formed (Table 3). The protons (–C10H10) and (–C13H13) of $(L^1)^{2-}$ unit are hydrogen bonded to two of ester oxygen (O2 and O7) atoms of $(L^1)^{2-}$ units, respectively, and the proton (–C11H11A) of the $(L^1)^{2-}$ unit is hydrogen bonded to one oxygen (O9) atom of the coordinated ethanol molecule. Meanwhile, the proton (–C25H25B) of the coordinated ethanol molecule is hydrogen bonded to one phenoxo oxygen (O6) atom of the $(L^1)^{2-}$ unit. The formation of intramolecular hydrogen bonds may result in a relatively stable chemical property of complex **1** [57,58].

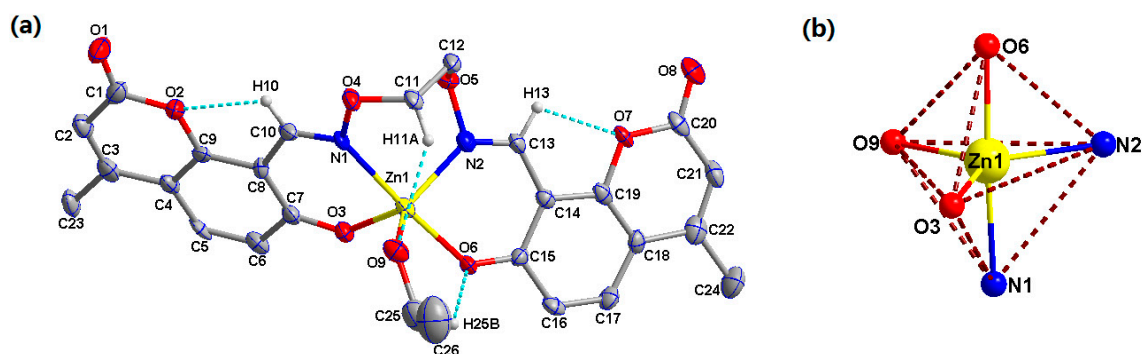


Figure 2. (a) Molecular structure and atom numberings of complex **1** with 30% probability displacement ellipsoids (hydrogen atoms are omitted for clarity). (b) Coordination polyhedron for Zn(II) ion of complex **1**.

Table 2. Selected bond lengths (Å) and angles (°) for complex **1**.

Bond			
Zn1–O3	1.940(5)	Zn1–N1	2.187(7)
Zn1–O6	1.994(5)	Zn1–N2	2.036(7)
Zn1–O9	2.049(6)		
Angles			
O3–Zn1–O6	97.1(2)	O3–Zn1–O9	111.5(2)
O3–Zn1–N1	86.7(2)	O3–Zn1–N2	125.1(3)
O6–Zn1–O9	91.7(2)	O6–Zn1–N1	175.8(2)
O6–Zn1–N2	87.0(2)	N1–Zn1–O9	88.5(3)
N2–Zn1–O9	123.2(3)	N2–Zn1–N1	89.4(3)

Table 3. Hydrogen bonding and C–H⋯ π stacking interactions (Å, °) for complex **1**.

D–H⋯A	D–H	H⋯A	D⋯A	D–H⋯A
C10–H10⋯O2	0.93	2.30	2.670(11)	103
C11–H11A⋯O9	0.97	2.59	3.421(10)	143
C13–H13⋯O7	0.93	2.25	2.636(10)	104
C25–H25B⋯O6	0.97	2.46	3.055(14)	119
C2–H2⋯O4	0.93	2.58	3.454(12)	158
C11–H11B⋯O8	0.97	2.49	3.281(9)	139
C12–H12A⋯O1	0.97	2.51	3.424(12)	157
C12–H12B⋯O3	0.97	2.56	3.494(11)	161
C21–H21⋯O3	0.93	2.54	3.277(11)	137
O9–H9⋯O8	0.86	1.99	2.725(10)	144
C26–H26B⋯Cg3	0.96	2.99	3.398(17)	107

Note: Cg3 = O₂–C₁–C₂–C₃–C₄–C₉.

As shown in Figure 3 and Table 3, six pairs of intermolecular hydrogen bonds, O9–H9⋯O8, C2–H2⋯O4, C11–H11B⋯O8, C12–H12A⋯O1, C12–H12B⋯O3, and C21–H21⋯O3 are formed. In addition, the Cg3 (O₂–C₁–C₂–C₃–C₄–C₉) of pyrone rings as acceptors forms one hydrogen bond with the protons (–C26H26B) of coordinated ethanol molecules. The space skeleton of complex **1** adopts a 3D supramolecular structure by the action of hydrogen bond and C–H⋯ π stacking interactions [34,59,60].

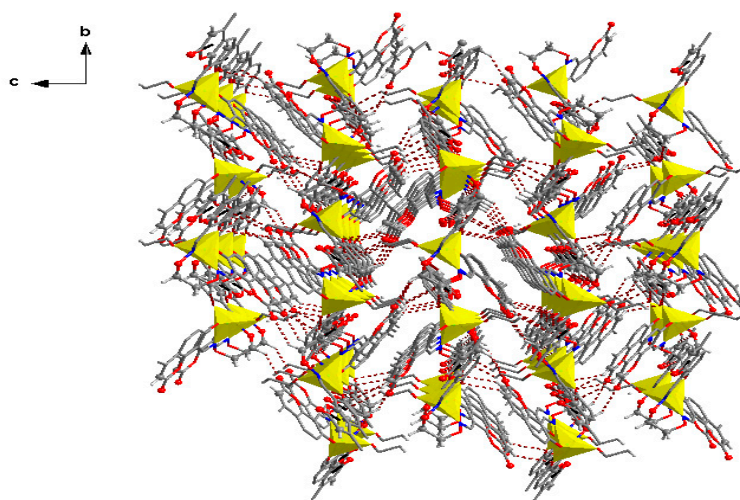


Figure 3. View of the 3D supramolecular structure of complex **1** showing the O-H...O, C-H...O, hydrogen bonds, and C-H... π stacking interactions.

3.3. Crystal Structure of Complex 2

X-ray crystallographic analysis of complex **2** reveals an asymmetric trinuclear structure. It crystallizes in the triclinic system, space group $P\bar{1}$, consists of three Zn(II) ions, two completely deprotonated $(L^2)^{1-}$ units, four coordinated acetate ions. Selected bond lengths and angles are listed in Table 4.

Table 4. Selected bond lengths (Å) and angles (°) for complex **2**.

Bond			
Zn1-O2	2.017(4)	Zn1-O9	2.203(4)
Zn1-O10	2.191(5)	Zn1-O11	2.112(4)
Zn1-N1	2.218(5)	Zn1-N2	2.077(5)
Zn2-O1	2.269(4)	Zn2-O2	2.006(4)
Zn2-O5	2.336(4)	Zn2-O6	2.001(4)
Zn2-O12	2.032(4)	Zn2-O13	2.022(4)
Zn3-O6	2.006(4)	Zn3-O14	2.147(4)
Zn3-O15	2.209(5)	Zn3-O16	2.160(5)
Zn3-N3	2.206(5)	Zn3-N4	2.085(5)
Angles			
O2-Zn1-O9	155.36(16)	O2-Zn1-O10	96.75(16)
O2-Zn1-O11	95.76(15)	O2-Zn1-N1	81.53(17)
O2-Zn1-N2	99.03(17)	O9-Zn1-N1	94.48(18)
O10-Zn1-O9	59.04(16)	O10-Zn1-N1	93.23(19)
O11-Zn1-O9	89.09(16)	O11-Zn1-O10	89.72(18)
O11-Zn1-N1	176.21(18)	N2-Zn1-O9	105.28(18)
N2-Zn1-O10	164.21(18)	N2-Zn1-O11	88.08(17)
N2-Zn1-N1	89.72(18)	O1-Zn2-O5	84.12(15)
O2-Zn2-O1	74.99(15)	O2-Zn2-O5	85.59(16)
O2-Zn2-O12	97.76(16)	O2-Zn2-O13	100.51(15)
O6-Zn2-O1	84.90(16)	O6-Zn2-O2	152.58(15)
O6-Zn2-O5	73.79(16)	O6-Zn2-O12	101.12(15)
O6-Zn2-O13	96.80(16)	O12-Zn2-O1	91.08(15)
O12-Zn2-O5	173.26(15)	O13-Zn2-O1	171.40(15)
O13-Zn2-O5	88.25(16)	O13-Zn2-O12	96.84(15)
O6-Zn3-O14	92.82(15)	O6-Zn3-O15	95.64(16)
O6-Zn3-O16	155.32(16)	O6-Zn3-N3	82.60(17)
O6-Zn3-N4	99.71(18)	O14-Zn3-O15	88.68(17)
O14-Zn3-O16	88.30(16)	O14-Zn3-N3	174.96(19)
O16-Zn3-O15	59.72(16)	O16-Zn3-N3	96.74(19)
N3-Zn3-O15	93.87(19)	N4-Zn3-O14	88.59(17)
N4-Zn3-O15	164.52(19)	N4-Zn3-O16	104.96(18)
N4-Zn3-N3	90.08(19)		

As shown in Figure 4, the two terminal Zn(II) ions (Zn1 and Zn3) were both located in the cis- N_2O coordination cavity of the deprotonated $(L^2)^{1-}$ units, the carboxylate oxygen (O9 and O10) and (O15 and O16) atoms from coordinated acetate ions chelate to Zn1 and Zn3, and carboxylate oxygen (O11 and O14) atoms from the μ_2 -acetate bridge to Zn1 and Zn3 in axial positions (Figure 4a). The dihedral angle between the coordination planes of O10–Zn1–O2 and N2–Zn1–O9 is 4.18(2), the dihedral angle between the coordination planes of N4–Zn3–O16 and N6–Zn3–O15 is 2.12(2), indicating slight distortion octahedral geometry from the square planar structure. Then, the coordination sphere of the central Zn(II) (Zn2) atom is completed by double μ_2 -phenoxo oxygen (O2 and O6) atoms from two $(L^2)^{1-}$ moieties, two μ_2 -acetato oxygen (O12 and O13) atoms and two oxygen (O5 and O1) atoms from methoxyl groups. As a result the central Zn2 atom finally has an $O_2O_2O_2$ coordination environment. Then, all of the hexa-coordinated Zn(II) ions of complex 2 have slightly distorted octahedral symmetries (Figure 4b) [61,62].

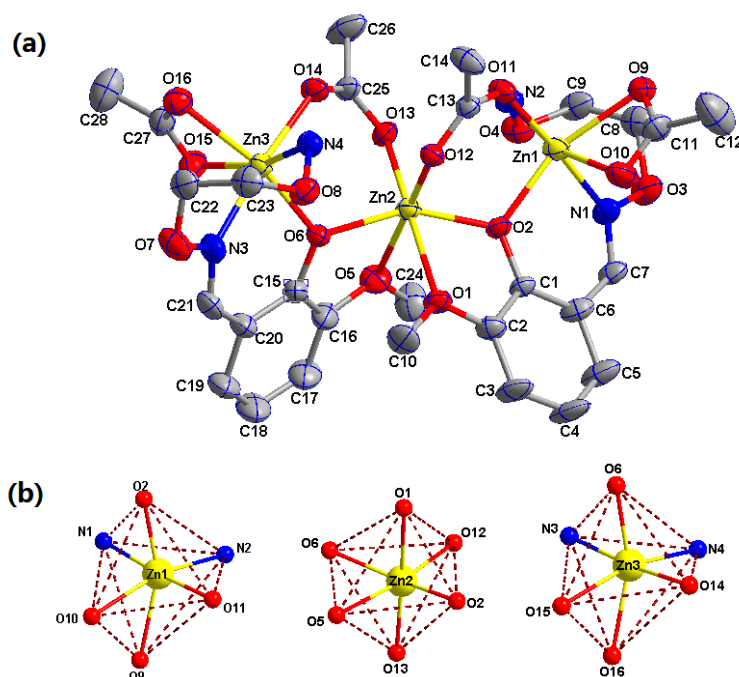


Figure 4. (a) Molecular structure and atom numberings of complex 2 with 30% probability displacement ellipsoids (hydrogen atoms are omitted for clarity). (b) Coordination polyhedra for Zn1, Zn2, and Zn3 ions of complex 2.

As depicted in Figure 5, in complex 2, four pairs of intramolecular hydrogen bonds N2–H2A...O13, N4–H4A...O12, C8–H8B...O9 and C22–H22B...O16 are formed. The protons (–N2H2A and –N4H4A) of $(L^2)^{1-}$ units form hydrogen bonds with two oxygen (O13 and O12) atoms of μ_2 -acetate ions, respectively. The protons (–C8H8B and –C22H22B) from ethylenedioxi carbon atoms of $(L^2)^{1-}$ units form hydrogen bonds with carboxylate oxygen (O9 and O16) atoms of coordinated acetate ions [63].

As illustrated in Figure 6 and Table 5, a large number of intermolecular hydrogen bonds and C–Cl... π , C–H... π stacking interactions in complex 2. The 2D supramolecular structure of complex 2 is composed of two parts. The first part was linked by intermolecular N2–H2B...O9, N4–H4B...O16 and C29–H29...O15 [41,64] hydrogen bonding interactions. The other part was made up of the C–Cl... π [27], C–H... π stacking interactions. The Cg7 (C15–C20) and Cg6 (C1–C6) of phenyl rings as acceptors form two hydrogen bonds with the protons (–C29Cl2 and –C10H10B) of adjacent molecules. The intermolecular hydrogen bonds and C–Cl... π , C–H... π stacking interactions of complex 2 not only make its spatial structure more diversified, but also may cause better chemical stability [27,59].

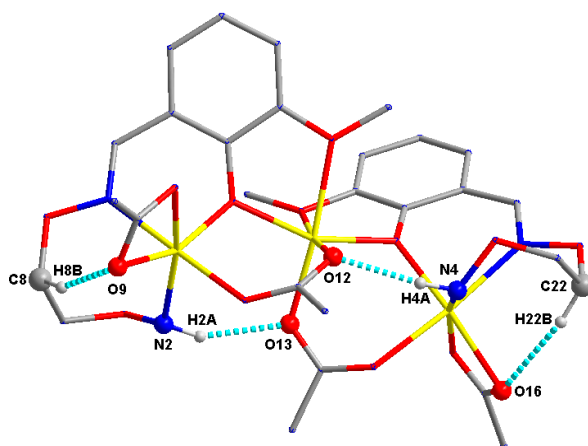


Figure 5. Intramolecular C-H...O and N-H...O hydrogen bonds of complex **2** (hydrogen atoms, except those forming hydrogen bonds, are omitted for clarity).

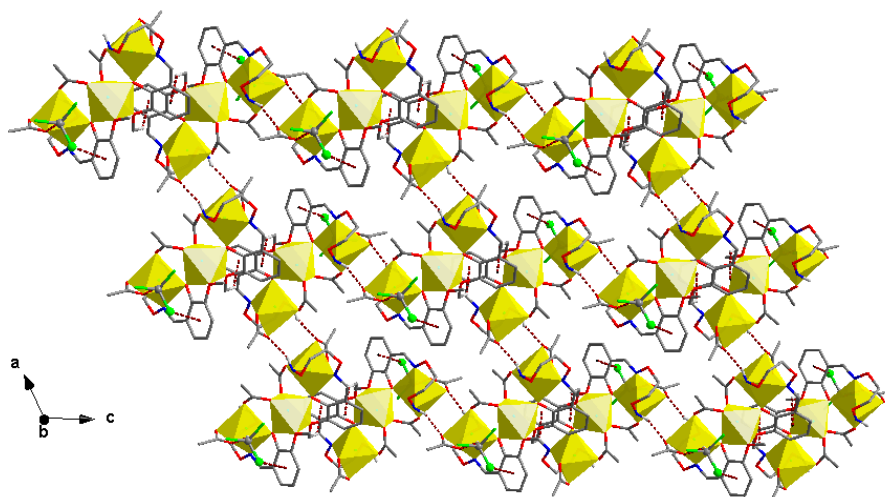


Figure 6. View of the 2D supramolecular structure of complex **2** showing the N-H...O, C-H...O hydrogen bonding, and C-Cl... π , C-H... π stacking interactions.

Table 5. Hydrogen bonding and C-H... π and C-Cl... π interactions (\AA , $^\circ$) for complex **2**.

D-H...A	D-H	H...A	D...A	D-H...A
N2-H2A ...O13	0.90	2.06	2.890(7)	153
N4-H4A...O12	0.90	2.10	2.945(8)	155
C8-H8B...O9	0.90	2.03	2.860(7)	154
C22-H22B ...O16	0.90	2.13	2.965(8)	153
N2-H2B ...O9	0.97	2.33	3.253(9)	158
N4-H4B ...O16	0.97	2.38	3.300(8)	157
C29-H29...O15	0.98	2.35	3.19(2)	145
N2-H2A ...O13	0.90	2.06	2.890(7)	153
C29-Cl2...Cg7	1.687	3.979	4.652(18)	102.7
C10-H10B ...Cg6	0.96	2.69	3.481(9)	140

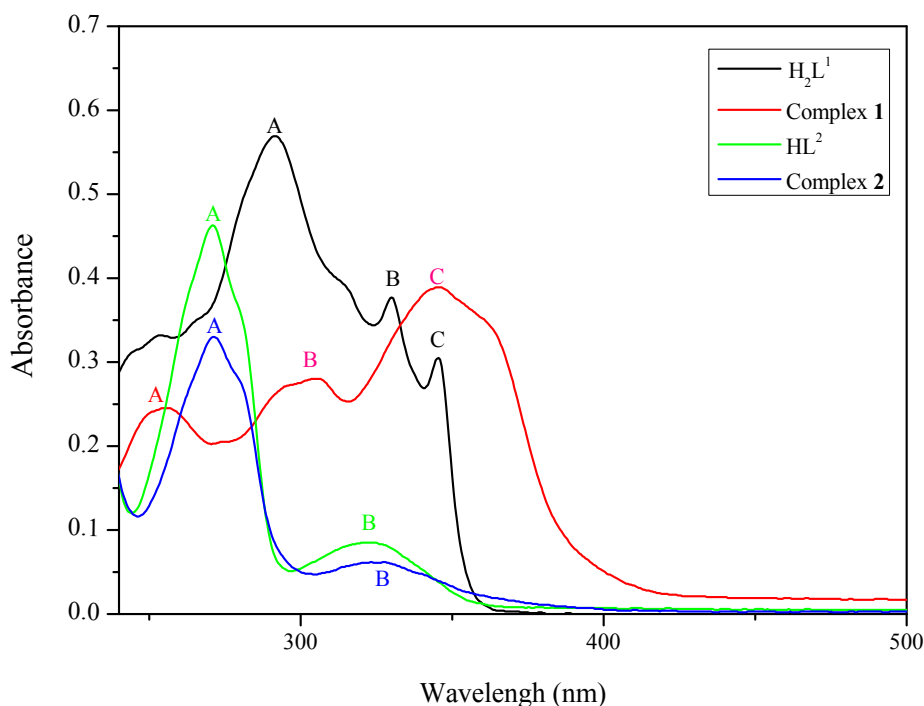
Note: Cg7 = C₁₅–C₂₀; Cg6=C₁–C₆.

3.4. UV-VIS Spectra

The UV-VIS absorption spectra of the free ligands H₂L¹ and HL² with their corresponding complexes **1** and **2** in the dichloromethane solutions (1.0×10^{-5} mol/L) at 298 K are shown in Table 6 and Figure 7.

Table 6. Absorption maxima and molar extinction coefficients for complexes **1** and **2**.

Compound	c	A(ϵ)	B(ϵ)	C(ϵ)
H ₂ L ¹	1.0×10^{-5}	291 (5.7×10^{-4})	329 (3.7×10^{-4})	345 (3.0×10^{-4})
Complex 1	1.0×10^{-5}	252 (2.4×10^{-4})	304 (2.8×10^{-4})	344 (3.9×10^{-4})
HL ²	1.0×10^{-5}	270 (4.6×10^{-4})	322 (0.8×10^{-4})	
Complex 2	1.0×10^{-5}	271 (3.3×10^{-4})	325 (0.6×10^{-4})	

**Figure 7.** The UV-VIS spectra of the free ligands H₂L¹ and HL² with their corresponding complexes **1** and **2** (cm^{−1}).

Obviously, the absorption peaks of the ligand H₂L¹ and HL² differ from those of their corresponding complexes **1** and **2**. The absorption spectrum of the free salamo-type ligand H₂L¹ consists of three relatively intense bands centered at 291, 329 and 345 nm, which may be assigned to the π - π^* transitions of the phenyl rings of coumarin and the oxime group [44,65]. Upon coordination of the ligand, the absorption intensities are weakened compared with the free ligand H₂L¹, which indicate that the oxime nitrogen atoms are involved in coordination to the Zn(II) atoms. Likewise, the absorption spectrum of the half-salamo ligand HL² consists of two relatively intense bands centred at 271 and 323 nm, which may be assigned to the π - π^* transitions of the phenyl rings and the oxime group [45,65]. On the other hand, because of complex **2** is synthesized by the half-salamo ligand HL², when the Zn(II) atoms coordinated to HL², the conjugate system of complex **2** not change greatly compared with complex **1**, which leads to the absorption spectra were almost unchanged before and after the complexation. Upon coordination of the ligand HL², the absorption intensities are weakened compared with the free ligand HL², which indicate that the oxime nitrogen atoms are involved in coordination with the Zn(II) atoms [37,66].

3.5. Fluorescence Properties

The fluorescence titration experiments of H₂L¹ and HL² were determined in DMF solution (2.0×10^{-5} mol·L^{−1}) with Zn(OAc)₂·2H₂O in methanol solution (1×10^{-3} mol·L^{−1}) are shown in Figures 8 and 9.

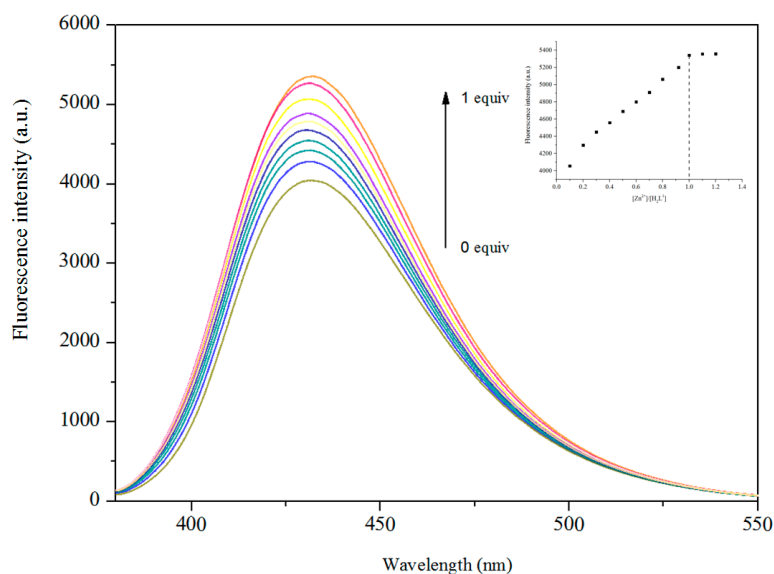


Figure 8. Absorption spectra of H_2L^1 in DMF solution upon the addition of Zn^{2+} . Inset: The absorbance at 432 nm varied as an interaction of $[Zn^{2+}]/[H_2L^1]$.

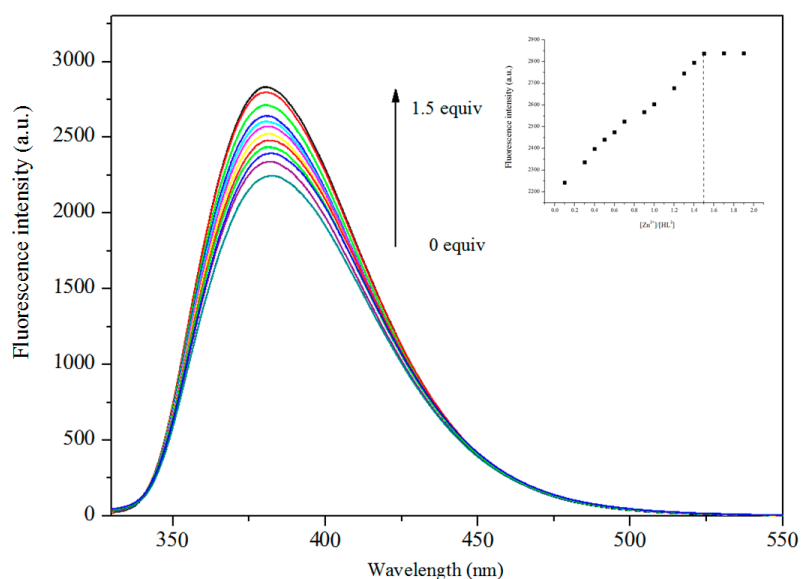


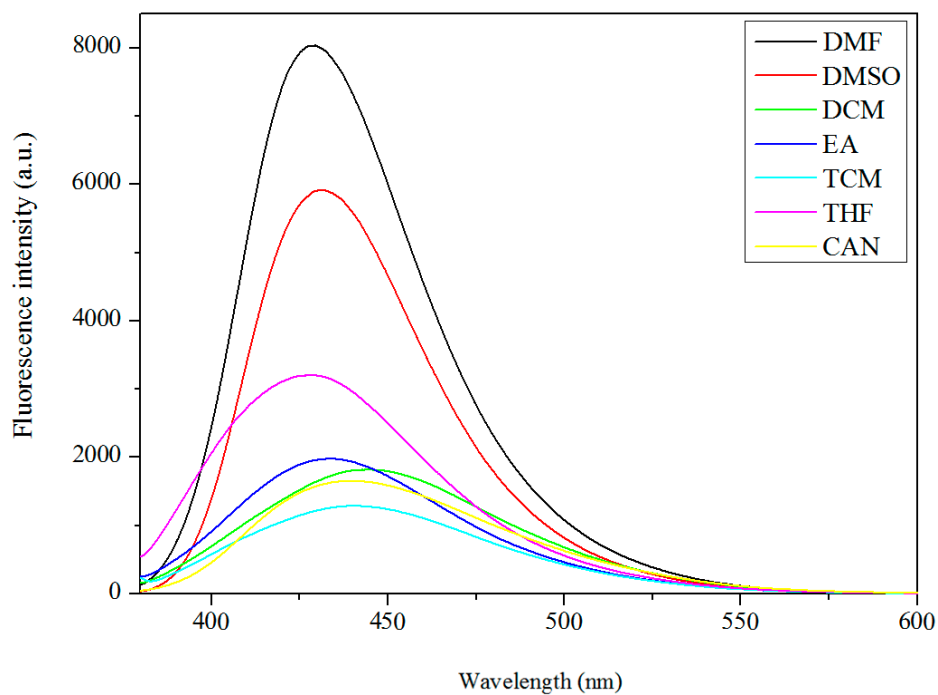
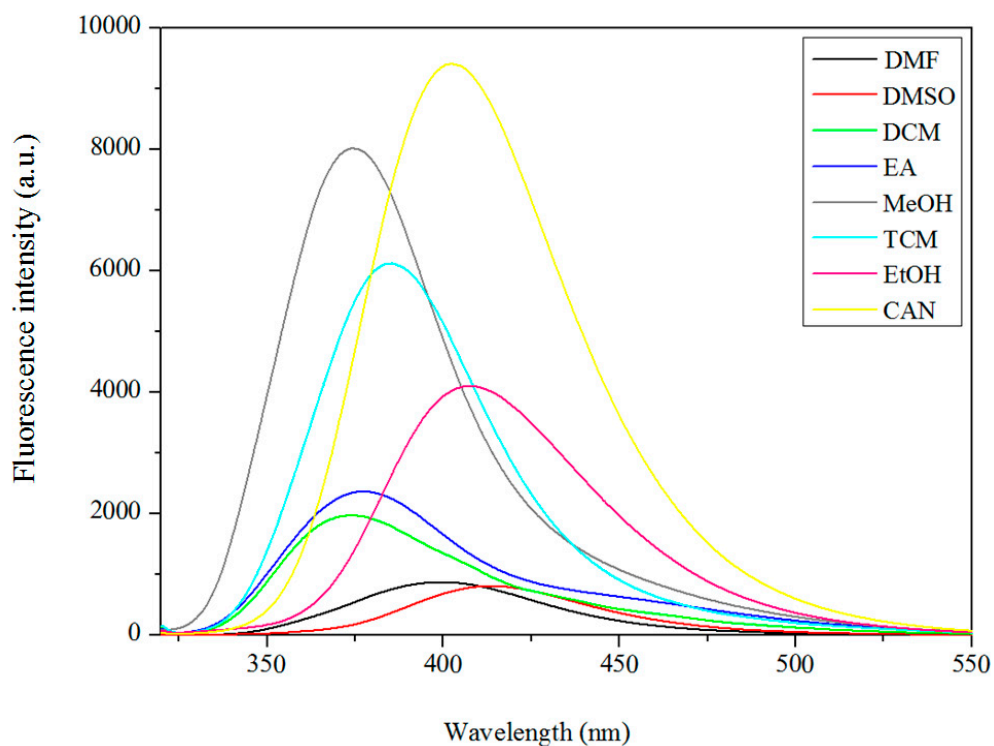
Figure 9. Absorption spectra of HL^2 in DMF solutions upon the addition of Zn^{2+} . Inset: The absorbance at 380 nm varied as an interaction of $[Zn^{2+}]/[HL^2]$.

The free ligand H_2L^1 appears as an intense emission peak at 432 nm. With the fluorescence titration experiment, upon the addition of Zn^{2+} , gradual changes in the fluorescence spectra. And the fluorescence intensity increased significantly. When the added amount of Zn^{2+} reached 1.0 equiv., the fluorescence emission intensity became stable, which indicates a 1:1 stoichiometry between Zn^{2+} and H_2L^1 . The enhancement of fluorescence is due to the coordination of metal ions with ligands [67]. Likewise, Complex 2 displays enhanced emission intensities compared to the corresponding ligand (HL^2) when excited at 380 nm. When the added amount of Zn^{2+} reached 1.5 equiv., the fluorescence emission intensity became steady. The result is corresponding to the crystal structure of complex 2 [68].

For research the solvent effect in fluorescence spectra of complexes 1 and 2, the fluorescence spectra of complex 1 and 2 in a series of solvents were examined and are shown in Table 7 and Figures 10 and 11.

Table 7. The maximum fluorescence emission in difference solvents for complexes 1 and 2.

Compound	DMF	DMSO	DCM	EA	TCM	CAN	THF	MeOH	EtOH
Complex 1	429	431	440	433	439	439	428		
Complex 2	399	414	372	377	384	402		373	407

**Figure 10.** The fluorescent ($\lambda_{\text{ex}} = 370 \text{ nm}$) spectra of complex 1 ($2.5 \times 10^{-5} \text{ M}$) in various solvents.**Figure 11.** The fluorescent ($\lambda_{\text{ex}} = 315 \text{ nm}$) spectra of complex 2 ($2.5 \times 10^{-5} \text{ M}$) in various solvents.

The normalized fluorescent spectra of complexes **1** and **2** are shown in Figures 12 and 13. Additionally, the fluorescence image of complexes **1** and **2** upon irradiation with a 365 nm UV lamp also indicated that the metal complexes **1** and **2** have promising applications as fluorescent materials. The solvent effect brings pivotal effect to the photoluminescence of complexes **1** and **2**.

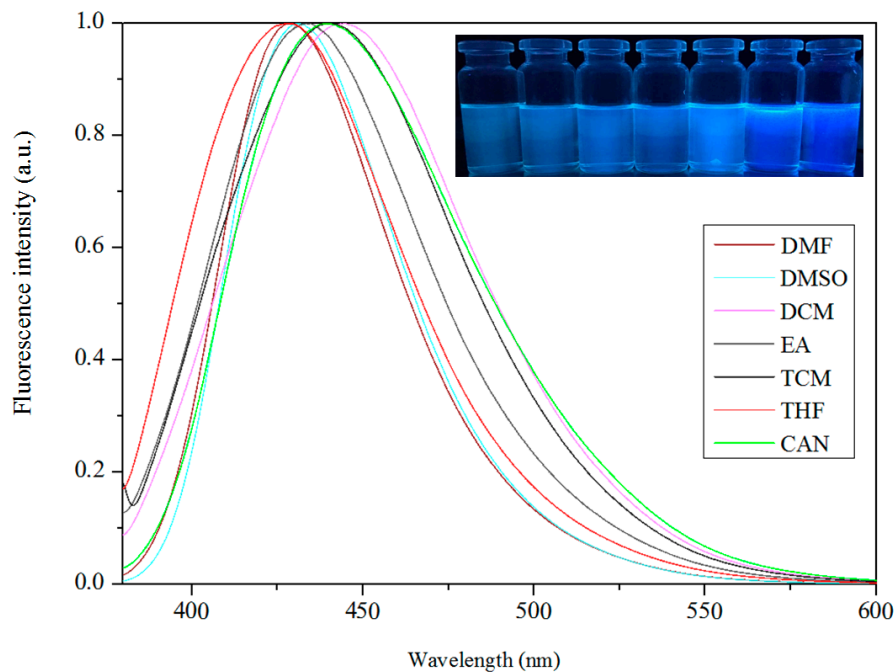


Figure 12. The normalized fluorescent spectra of complex **1**. Inset image: the fluorescence picture of complex **1** in various solvents upon irradiation with a 365 nm UV lamp.

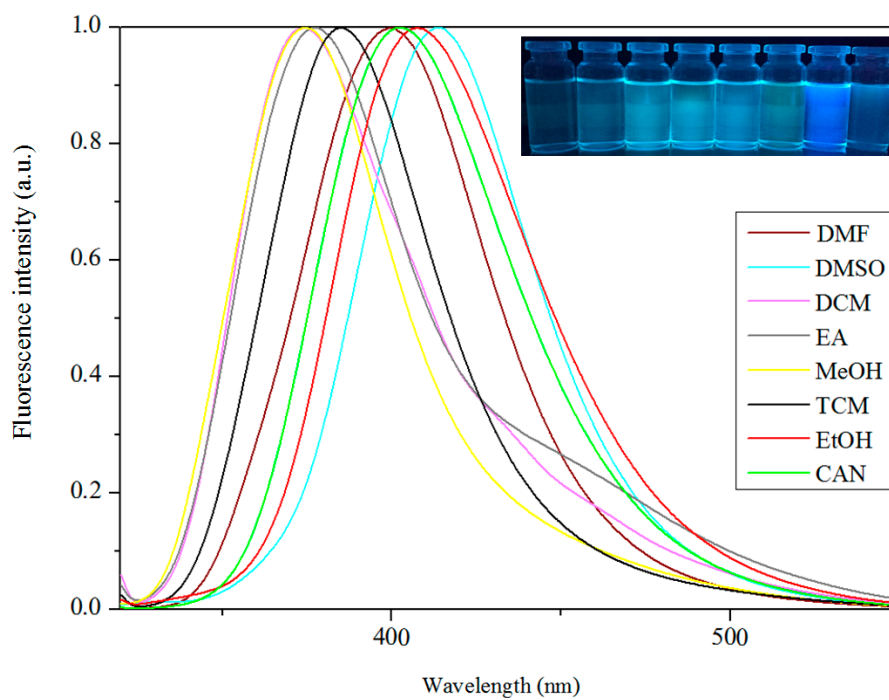


Figure 13. The normalized fluorescent spectra of complex **2**. Inset image: the fluorescence picture of complex **1** in various solvents upon irradiation with a 365 nm UV lamp.

As we know, many fluorescent complexes, especially those containing polar substituents on aromatic rings, are susceptible to solvents [27]. Due to the difference in polarity of solvents, complex **1** exhibits the relatively strong maximum fluorescence emission with relatively low solvent polarity in TCM and DCM at 439 and 440 nm, respectively. Additionally, in solvents THF, DMF, and DMSO with higher solvent polarity, the maximum fluorescence emission is relatively weak at 428, 429, and 431 nm, respectively. In solvents of medium polarity, EA and CAN, the maximum fluorescence emission was at 433 and 439 nm, respectively. Meanwhile, complex **2** exhibits the relatively strong maximum fluorescence emission with relatively high solvent polarity in DMF, CAN, EtOH, and DMSO at 399, 402, 407, and 414 nm, respectively. In solvents DCM, TCM, and EA with lower solvent polarity, the maximum fluorescence emission is relatively weak at 372, 384 and 377 nm, respectively. Furthermore, the maximum fluorescence emission unusually appears at 373 nm in MeOH solvent. The influence of the solvent effect changes the luminescent properties of complexes **1** and **2**, making its application areas broad [27,69].

4. Conclusions

In summary, we have reported the successful syntheses and characterizations of two newly-designed complexes, $[\text{Zn}(\text{L}^1)(\text{EtOH})]$ (**1**) and $[\{\text{Zn}(\text{L}^2)(\text{OAc})_2\}_2\text{Zn}]\cdot\text{CHCl}_3$ (**2**), derived from salamo and half-salamo chelating ligands (H_2L^1 and HL^2). Complex **1** includes one Zn(II) ion, one completely deprotonated $(\text{L}^1)^{2-}$ unit and one coordinated ethanol molecule, which shows a slightly distorted trigonal bipyramidal geometry and forms an infinite 3D supramolecular structure. Complex **2** includes three Zn(II) ions, two completely deprotonated $(\text{L}^2)^{1-}$ moieties, four coordinated acetate ions, and possesses an infinite 2D space structure. The normalized fluorescent spectra exhibit that complexes **1** and **2** have favourable fluorescent emissions in different solvents.

Acknowledgments: This work was supported by the National Natural Science Foundation of China (21361015, 21761018), the Outstanding Research Platform (Team), and the Graduate Student Guidance Team Building Fund of Lanzhou Jiaotong University (260001), which are gratefully acknowledged.

Author Contributions: Wen-Kui Dong and Lei Gao conceived and designed the experiments; Fei Wang performed the experiments; Yang Zhang analyzed the data; Wen-Kui Dong contributed reagents/materials/analysis tools; Xiu-Yan Dong wrote the paper.

Conflicts of Interest: The authors declare no competing financial interests.

References

1. Dong, W.K.; Lan, P.F.; Zhou, W.M.; Zhang, Y. Salamo-type trinuclear and tetranuclear cobalt(II) complexes based on a new asymmetry salamo-type ligand: Syntheses, crystal structures and fluorescence properties. *J. Coord. Chem.* **2016**, *65*, 1272–1283. [[CrossRef](#)]
2. Dong, X.Y.; Akogun, S.F.; Zhou, W.M.; Dong, W.K. Tetranuclear Zn(II) complex based on an asymmetrical Salamo-type chelating ligand: Synthesis, structural characterization, and fluorescence property. *J. Chin. Chem. Soc.* **2017**, *64*, 412–419. [[CrossRef](#)]
3. Tao, C.H.; Ma, J.C.; Zhu, L.C.; Zhang, Y.; Dong, W.K. Heterobimetallic 3d–4f Zn(II)–Ln(III) (Ln = Sm, Eu, Tb and Dy) complexes with a N_2O_4 bisoxime chelate ligand and a simple auxiliary ligand Py: Syntheses, structures and luminescence properties. *Polyhedron* **2017**, *128*, 38–45. [[CrossRef](#)]
4. Dong, Y.J.; Dong, X.Y.; Dong, W.K.; Zhang, Y.; Zhang, L.S. Three asymmetric Salamo-type copper(II) and cobalt(II) complexes: Syntheses, structures, fluorescent properties. *Polyhedron* **2017**, *123*, 305–315. [[CrossRef](#)]
5. Dong, W.K.; Ma, J.C.; Dong, Y.J.; Zhao, L.; Zhu, L.C.; Sun, Y.X.; Zhang, Y. Two hetero-trinuclear Zn(II)–M(II) (M = Sr, Ba) complexes based on metallohost of mononuclear Zn(II) complex: Syntheses, structures and fluorescence properties. *J. Coord. Chem.* **2016**, *69*, 3231–3241. [[CrossRef](#)]
6. Wu, H.L.; Wang, C.P.; Wang, F.; Peng, H.P.; Zhang, H.; Bai, Y.C. A new manganese(III) complex from bis(5-methylsalicylaldehyde)-3-oxapentane-1,5-diamine: Synthesis, characterization, antioxidant activity and luminescence. *J. Chin. Chem. Soc.* **2015**, *62*, 1028–1034. [[CrossRef](#)]

7. Wu, H.L.; Bai, Y.C.; Zhang, Y.H.; Li, Z.; Wu, M.C.; Chen, C.Y.; Zhang, J.W. Synthesis, crystal structure, antioxidation and DNA-binding properties of a dinuclear copper(II) complex with bis(*N*-salicylidene)-3-oxapentane-1, 5-diamine. *J. Coord. Chem.* **2014**, *67*, 3054–3066. [[CrossRef](#)]
8. Wu, H.L.; Bai, Y.; Yuan, J.K.; Wang, H.; Pan, G.L.; Fan, X.Y.; Kong, J. A zinc(II) complex with tris(2-(*N*-methyl)benzimidazylmethyl)amine and salicylate: Synthesis, crystal structure, and DNA-binding. *J. Coord. Chem.* **2012**, *65*, 2839–2851. [[CrossRef](#)]
9. Wu, H.L.; Pan, G.L.; Wang, H.; Wang, X.L.; Bai, Y.C.; Zhang, Y.H. Study on synthesis, crystal structure, antioxidant and DNA-binding of mono-, di- and poly-nuclear lanthanides complexes with bis(*N*-salicylidene)-3-oxapentane-1,5-diamine. *J. Photochem. Photobiol. B Biol.* **2014**, *135*, 33–43. [[CrossRef](#)] [[PubMed](#)]
10. Wu, H.L.; Bai, Y.C.; Zhang, Y.H.; Pan, G.L.; Kong, J.; Shi, F.; Wang, X.L. Two lanthanide(III) complexes based on the schiff base *N,N*-Bis(salicylidene)-1,5-diamino-3-oxapentane: Synthesis, characterization, DNA-binding properties, and antioxidation. *Z. Anorg. Allg. Chem.* **2014**, *640*, 2062–2071. [[CrossRef](#)]
11. Wu, H.L.; Pan, G.L.; Bai, Y.C.; Wang, H.; Kong, J.; Shi, F.; Zhang, Y.H.; Wang, X.L. Preparation, structure, DNA-binding properties, and antioxidant activities of a homodinuclear erbium(III) complex with a pentadentate Schiff base ligand. *J. Chem. Res.* **2014**, *38*, 211–217. [[CrossRef](#)]
12. Wu, H.L.; Pan, G.L.; Bai, Y.C.; Wang, H.; Kong, J. Synthesis, structure, antioxidation, and DNA-binding studies of a binuclear ytterbium(III) complex with bis(*N*-salicylidene)-3-oxapentane-1,5-diamine. *Res. Chem. Intermed.* **2015**, *41*, 3375–3388. [[CrossRef](#)]
13. Chen, C.Y.; Zhang, J.W.; Zhang, Y.H.; Yang, Z.H.; Wu, H.L. Gadolinium(III) and dysprosium(III) complexes with a Schiff base bis(*N*-salicylidene)-3-oxapentane-1,5-diamine: Synthesis, characterization, antioxidation, and DNA-binding studies. *J. Coord. Chem.* **2015**, *68*, 1054–1071. [[CrossRef](#)]
14. Dong, W.K.; Ma, J.C.; Zhu, L.C.; Zhang, Y.; Li, X.L. Four new nickel(II) complexes based on an asymmetric Salamo-type ligand: Synthesis, structure, solvent effect and electrochemical property. *Inorg. Chim. Acta* **2016**, *445*, 140–148. [[CrossRef](#)]
15. Chai, L.Q.; Zhang, K.Y.; Tang, L.J.; Zhang, J.Y.; Zhang, H.S. Two mono- and dinuclear ni(II) complexes constructed from quinazoline-type ligands: Synthesis, x-ray structures, spectroscopic, electrochemical, thermal, and antimicrobial studies. *Polyhedron* **2017**, *130*, 100–107. [[CrossRef](#)]
16. Yu, T.Z.; Zhang, K.; Zhao, Y.L.; Yang, C.H.; Zhang, H.; Qian, L.; Fan, D.W.; Dong, W.K.; Chen, L.L.; Qiu, Y.Q. Synthesis, crystal structure and photoluminescent properties of an aromatic bridged Schiff base ligand and its zinc complex. *Inorg. Chim. Acta* **2008**, *361*, 233–240. [[CrossRef](#)]
17. Dong, Y.J.; Ma, J.C.; Zhu, L.C.; Dong, W.K.; Zhang, Y. Four 3d–4f heteromultinuclear zinc(II)–lanthanide(III) complexes constructed from a distinct hexadentate N₂O₂-type ligand: Syntheses, structures and photophysical properties. *J. Coord. Chem.* **2017**, *70*, 103–115. [[CrossRef](#)]
18. Wang, L.; Ma, J.C.; Dong, W.K.; Zhu, L.C.; Zhang, Y. A novel Self-assembled nickel(II)–cerium(III) heterotetranuclear dimer constructed from N₂O₂-type bisoxime and terephthalic acid: Synthesis, structure and photophysical properties. *Z. Anorg. Allg. Chem.* **2016**, *642*, 834–839. [[CrossRef](#)]
19. Dong, W.K.; Chen, X.; Sun, Y.X.; Yang, Y.H.; Zhao, L.; Xu, L.; Yu, T.Z. Synthesis, structure and spectroscopic properties of two new trinuclear nickel(II) clusters possessing solvent effect. *Spectrochim. Acta Part A* **2009**, *74*, 719–725. [[CrossRef](#)] [[PubMed](#)]
20. Dong, W.K.; Li, G.; Wang, Z.K.; Dong, X.Y. A novel trinuclear cobalt(II) complex derived from an asymmetric Salamo-type N₂O₃ bisoxime chelate ligand: Synthesis, structure and optical properties. *Spectrochimica Acta Part A* **2014**, *133*, 340–347. [[CrossRef](#)] [[PubMed](#)]
21. Liu, Y.A.; Wang, C.Y.; Zhang, M.; Song, X.Q. Structures and magnetic properties of cyclic heterometallic tetranuclear clusters. *Polyhedron* **2017**, *127*, 278–286. [[CrossRef](#)]
22. Dong, W.K.; Ma, J.C.; Dong, Y.J.; Zhu, L.C.; Zhang, Y. Di- and tetranuclear heterometallic 3d–4f cobalt(II)–lanthanide(III) complexes derived from a hexadentate bisoxime: Syntheses, structures and magnetic properties. *Polyhedron* **2016**, *115*, 228–235. [[CrossRef](#)]
23. Song, X.Q.; Liu, P.P.; Xiao, Z.R.; Li, X.; Liu, Y.A. Four polynuclear complexes based on a versatile salicylamide salen-like ligand: Synthesis, structural variations and magnetic properties. *Inorg. Chim. Acta* **2015**, *438*, 232–244. [[CrossRef](#)]
24. Liu, P.P.; Wang, C.Y.; Zhang, M.; Song, X.Q. Pentanuclear sandwich-type Zn^{II}–Ln^{III} clusters based on a new Salen-like salicylamide ligand: Structure, near-infrared emission and magnetic properties. *Polyhedron* **2017**, *129*, 133–140. [[CrossRef](#)]

25. Dong, W.K.; Ma, J.C.; Zhu, L.C.; Zhang, Y. Nine self-assembled nickel(II)–lanthanide(III) heterometallic complexes constructed from a Salamo-type bisoxime and bearing N- or O-donor auxiliary ligand: Syntheses, structures and magnetic properties. *New J. Chem.* **2016**, *40*, 6998–7010. [[CrossRef](#)]
26. Dong, W.K.; Ma, J.C.; Zhu, L.C.; Zhang, Y. Self-assembled zinc(II)-lanthanide(III) heteromultinuclear complexes constructed from 3-MeOsalamo ligand: Syntheses, structures and luminescent properties. *Cryst. Growth Des.* **2016**, *16*, 6903–6914. [[CrossRef](#)]
27. Chen, L.; Dong, W.K.; Zhang, H.; Zhang, Y.; Sun, Y.X. Structural variation and luminescence properties of tri- and dinuclear Cu^{II} and Zn^{II} complexes constructed from a naphthalenediol-based bis(Salamo)-type ligand. *Cryst. Growth Des.* **2017**, *17*, 3636–3648. [[CrossRef](#)]
28. Song, X.Q.; Peng, Y.J.; Chen, G.Q.; Wang, X.R.; Liu, P.P.; Xu, W.Y. Substituted group-directed assembly of Zn(II) coordination complexes based on two new structural related pyrazolone based Salen ligands: Syntheses, structures and fluorescence properties. *Inorg. Chim. Acta.* **2015**, *427*, 13–21. [[CrossRef](#)]
29. Dong, W.K.; Zhang, J.; Zhang, Y.; Li, N. Novel multinuclear transition metal(II) complexes based on an asymmetric Salamo-type ligand: Syntheses, structure characterizations and fluorescent properties. *Inorg. Chim. Acta.* **2016**, *444*, 95–102. [[CrossRef](#)]
30. Dong, W.K.; Akogun, S.F.; Zhang, Y.; Dong, X.Y. A reversible “turn-on” fluorescent sensor for selective detection of Zn²⁺. *Sensors Actuators B Chem.* **2017**, *238*, 723–734. [[CrossRef](#)]
31. Dong, Y.J.; Li, X.L.; Zhang, Y.; Dong, W.K. A highly selective visual and fluorescent sensor for Pb²⁺ and Zn²⁺ and crystal structure of Cu²⁺ complex based-on a novel single-armed Salamo-type bisoxime. *Supramol. Chem.* **2017**, *29*, 518–527. [[CrossRef](#)]
32. Dong, W.K.; Li, X.L.; Wang, L.; Zhang, Y.; Ding, Y.J. A new application of Salamo-type bisoximes: as a relay-sensor for Zn²⁺/Cu²⁺ and its novel complexes for successive sensing of H⁺/OH[−]. *Sens. Actuators B Chem.* **2016**, *229*, 370–378. [[CrossRef](#)]
33. Zhao, L.; Dang, X.T.; Chen, Q.; Zhao, J.X.; Wang, L. Synthesis, crystal structure and spectral properties of a 2D supramolecular copper(II) complex with 1-(4-[(E)-3-ethoxyl-2-hydroxybenzylidene]amino)phenyl)ethanone oxime. *Synth. React. Inorg. Met.-Org. Nano-Met. Chem.* **2013**, *43*, 1241–1246. [[CrossRef](#)]
34. Sun, Y.X.; Xu, L.; Zhao, T.H.; Liu, S.H.; Liu, G.H.; Dong, X.T. Synthesis and crystal structure of a 3D supramolecular copper(II) complex with 1-(3-[(E)-3-bromo-5-chloro-2-hydroxybenzylidene]amino)phenyl)ethanone oxime. *Synth. React. Inorg. Met.-Org. Nano-Met. Chem.* **2013**, *43*, 509–513. [[CrossRef](#)]
35. Sun, Y.X.; Dong, W.K.; Wang, L.; Zhao, L.; Yang, Y.H. Synthesis and crystal structure of nickel(II) cluster with salen-type bisoxime ligand. *Chinese J. Inorg. Chem.* **2009**, *25*, 1478–1482.
36. Sun, Y.X.; Zhang, S.T.; Ren, Z.L.; Dong, X.Y.; Wang, L. Synthesis, characterization, and crystal structure of a new supramolecular Cd^{II} complex with halogen-substituted salen-type bisoxime. *Synth. React. Inorg. Met.-Org. Nano-Met Chem.* **2013**, *43*, 995–1000. [[CrossRef](#)]
37. Dong, W.K.; Zhang, X.Y.; Zhao, M.M.; Li, G.; Dong, X.Y. Syntheses and crystal structures of 5-Methoxy-6'-hydroxy-2,2'-[ethylenedioxybis(nitrilomethylidyne)]diphenol and its tetranuclear zinc(II) complex. *Chin. J. Inorg. Chem.* **2014**, *30*, 710–716.
38. Zhou, J.A.; Tang, X.L.; Cheng, J.; Ju, Z.H.; Yang, L.Z.; Liu, W.S.; Chen, C.Y.; Bai, D.C. An 1,3,4-oxadiazole-based off-on fluorescent chemosensor for Zn²⁺ in aqueous solution and imaging application in living cells. *Dalton Trans.* **2012**, *41*, 10626–10632. [[CrossRef](#)] [[PubMed](#)]
39. Akine, S.; Taniguchi, T.; Dong, W.K.; Masubuchi, S.; Nabeshima, T. Oxime-Based Salen-Type Tetradentate Ligands with High Stability against Imine Metathesis Reaction. *J. Org. Chem.* **2005**, *70*, 1704–1711. [[CrossRef](#)] [[PubMed](#)]
40. Akine, S.; Dong, W.K.; Nabeshima, T. Octanuclear zinc(II) and cobalt(II) clusters produced by cooperative tetrameric assembling of oxime chelate ligands. *Inorg. Chem.* **2006**, *454*, 677–684. [[CrossRef](#)] [[PubMed](#)]
41. Song, X.Q.; Cheng, G.Q.; Liu, Y.A. Enhanced Tb(III) luminescence by d¹⁰ transition metal coordination. *Inorg. Chim. Acta* **2016**, *450*, 386–394. [[CrossRef](#)]
42. Darensbourg, D.J.; Karroonnirun, O.; Wilson, S.J. Ring-Opening Polymerization of Cyclic Esters and Trimethylene Carbonate Catalyzed by Aluminum Half-Salen Complexes. *Inorg. Chem.* **2011**, *50*, 6775–6787. [[CrossRef](#)] [[PubMed](#)]
43. Darensbourg, D.J.; Karroonnirun, O. Stereoselective Ring-Opening Polymerization of *rac*-Lactides Catalyzed by Chiral and Achiral Aluminum Half-Salen Complexes. *Organometallics* **2010**, *29*, 5627–5634. [[CrossRef](#)]

44. Dong, Y.; Li, F.J.; Jiang, X.X.; Song, F.Y.; Cheng, Y.X.; Zhu, C.J. Na⁺ triggered fluorescence sensors for Mg²⁺ detection based on a coumarin salen moiety. *Org. Lett.* **2011**, *9*, 2252–2255. [[CrossRef](#)] [[PubMed](#)]
45. Dong, W.K.; Wang, Z.K.; Li, G.; Zhao, M.M.; Dong, X.Y.; Liu, S.H. Syntheses, crystal structures, and properties of a Salamo-type tetradentate chelating ligand and its pentacoordinated copper(II) complex. *Z. Anorg. Allg. Chem.* **2013**, *639*, 2263–2268. [[CrossRef](#)]
46. Dong, W.K.; Feng, J.H.; Yang, X.Q. Synthesis and crystal structure of a five-coordinated cu(II) dimer with 4,4'-Dibromo-2,2'-[ethylenedioxybis(nitrilomethylidyne)]diphenol. *Synth. React. Inorg. Met. Org. Nano Met. Chem.* **2007**, *37*, 189–192. [[CrossRef](#)]
47. Ma, J.C.; Dong, X.Y.; Dong, W.K.; Zhang, Y.; Zhu, L.C.; Zhang, J.T. An unexpected dinuclear Cu(II) complex with a bis(Salamo) chelating ligand: synthesis, crystal structure, and photophysical properties. *J. Coord. Chem.* **2016**, *69*, 149–159. [[CrossRef](#)]
48. Sheldrick, G.M. SHELXS-97. In *Program for the Solution and the Refinement of Crystal Structures*; University of Gottingen: Germany, 1997.
49. Dong, W.K.; Zhang, F.; Li, N.; Xu, L.; Zhang, Y.; Zhang, J.; Zhu, L.C. Trinuclear cobalt(II) and zinc(II) salamo-type complexes: Syntheses, crystal structures, and fluorescent properties. *Z. Anorg. Allg. Chem.* **2016**, *642*, 532–538. [[CrossRef](#)]
50. Dong, W.K.; Zhang, L.S.; Sun, Y.X.; Zhao, M.M.; Li, G.; Dong, X.Y. Synthesis, crystal structure and spectroscopic properties of a supramolecular zinc(II) complex with N₂O₂ coordination sphere. *Spectrochim. Acta Part A* **2014**, *121*, 324–329. [[CrossRef](#)] [[PubMed](#)]
51. Hao, J.; Li, L.H.; Zhang, J.T.; Akogun, S.F.; Wang, L.; Dong, W.K. Four homo- and hetero-bimetallic 3d/3d-2s complexes constructed from a naphthalenediol-based acyclic bis(salamo)-type tetraoxime ligand. *Polyhedron* **2017**, *134*, 1–10. [[CrossRef](#)]
52. Li, L.H.; Dong, W.K.; Zhang, Y.; Akogun, S.F.; Xu, L. Syntheses, structures and catecholase activities of homo- and hetero-trinuclear cobalt(II) complexes constructed from an acyclic naphthalenediol-based bis(salamo)-type ligand. *Appl. Organomet. Chem.* [[CrossRef](#)]
53. Addison, A.W.; Rao, T.N.; Reedijk, J.; van Rijn, J.; Verschoor, G.C. Synthesis, structure, and spectroscopic properties of copper(II) compounds containing nitrogen–sulphur donor ligands; the crystal and molecular structure of aqua[1,7-bis(*N*-methylbenzimidazol-2'-yl)-2,6-dithiaheptane]copper(II) perchlorate. *J. Chem. Soc. Dalton Trans.* **1984**, *7*, 1349–1356. [[CrossRef](#)]
54. Konno, T.; Tokuda, K.; Sakurai, J.; Okamoto, K.I. Five-Coordinate Geometry of Cadmium(II) with Octahedral Bidentate-S,S Complex-Ligand cis(S)-[Co(aet)₂(en)]⁺ (aet = 2-aminoethanethiolate): Synthesis, Crystal Structures and Interconversion of S-Bridged Co^{III}Cd^{II} Polynuclear Complexes. *Bull. Chem. Soc. Jpn.* **2000**, *73*, 2767–2773. [[CrossRef](#)]
55. Chai, L.Q.; Tang, L.J.; Chen, L.C.; Huang, J.J. Structural, spectral, electrochemical and DFT studies of two mononuclear manganese(II) and zinc(II) complexes. *Polyhedron* **2017**, *122*, 228–240. [[CrossRef](#)]
56. Xu, L.; Zhu, L.C.; Ma, J.C.; Zhang, Y.; Zhang, J.; Dong, W.K. Syntheses, structures and spectral properties of mononuclear Cu^{II} and dimeric Zn^{II} complexes based on an asymmetric Salamo-type N₂O₂ ligand. *Z. Anorg. Allg. Chem.* **2015**, *641*, 2520–2524. [[CrossRef](#)]
57. Boggs, J.M. Lipid intermolecular hydrogen bonding: influence on structural organization and membrane function. *Biochim. Biophys. Acta* **1987**, *906*, 353–404. [[CrossRef](#)]
58. Karas, L.J.; Batista, P.R.; Viesser, R.V.; Tormena, C.F.; Rittner, R.; de Oliveira, P.R. Trends of intramolecular hydrogen bonding in substituted alcohols: a deeper investigation. *Phys. Chem. Chem. Phys.* **2017**, *19*, 16904–16913. [[CrossRef](#)] [[PubMed](#)]
59. Mathias, J.P.; Simanek, E.E.; Whitesides, G.M. Self-Assembly through Hydrogen Bonding: Peripheral Crowding-A new strategy for the preparation of stable supramolecular aggregates based on parallel, connected CA₃.cntdot.M₃ rosettes. *J. Am. Chem. Soc.* **1994**, *116*, 4326–4340.
60. Yabuuchi, K.; Marfo-Owusu, E.; Kato, T. A new urea gelator: incorporation of intra- and intermolecular hydrogen bonding for stable 1D self-assembly. *Org. Biomol. Chem.* **2003**, *1*, 3464–3469. [[CrossRef](#)] [[PubMed](#)]
61. Chai, L.Q.; Huang, J.J.; Zhang, J.Y.; Li, Y.X. Two 1-D and 2-D cobalt(II) complexes: Synthesis, crystal structures, spectroscopic and electrochemical properties. *J. Coord. Chem.* **2015**, *68*, 1224–1237. [[CrossRef](#)]
62. Sun, Y.X.; Wang, L.; Dong, X.Y.; Ren, Z.L.; Meng, W.S. Synthesis, characterization, and crystal structure of a supramolecular Co^{II} complex containing Salen-type bisoxime. *Synth. React. Inorg. Met.-Org. Nano-Met. Chem.* **2013**, *43*, 599–603. [[CrossRef](#)]

63. Wang, P.; Zhao, L. Synthesis and crystal structure of supramolecular copper(II) complex based on N_2O_2 coordination Sphere. *Asian J. Chem.* **2015**, *4*, 1424–1426. [[CrossRef](#)]
64. Liu, P.P.; Sheng, L.; Song, X.Q.; Xu, W.Y.; Liu, Y.A. Synthesis, structure and magnetic properties of a new one dimensional manganese coordination polymer constructed by a new asymmetrical ligand. *Inorg. Chim. Acta* **2015**, *434*, 252–257. [[CrossRef](#)]
65. Wang, B.J.; Dong, W.K.; Zhang, Y.; Akogun, S.F. A novel relay-sensor for highly sensitive and selective detection of Zn^{2+}/Pic^- and fluorescence on/off switch response of H^+/OH^- . *Sens. Actuators B Chem.* **2017**, *247*, 254–264. [[CrossRef](#)]
66. Akine, S.; Morita, Y.; Utsuno, F.; Nabeshima, T. Multiple folding structures mediated by metal coordination of acyclic multidentate ligand. *Inorg. Chem.* **2009**, *48*, 10670–10678. [[CrossRef](#)] [[PubMed](#)]
67. Song, X.Q.; Liu, P.P.; Liu, Y.A.; Zhou, J.J.; Wang, X.L. Two dodecanuclear heterometallic $[Zn_6Ln_6]$ clusters constructed by a multidentate salicylamide salen-like ligand: Synthesis, structure, luminescence and magnetic properties. *Dalton Trans.* **2016**, *45*, 8154–8163. [[CrossRef](#)] [[PubMed](#)]
68. Guo, C.Y.; Wang, Y.Y.; Xu, K.Z.; Zhu, H.L.; Liu, P.; Shi, Q.Z. Crystal structures, bioactivities and fluorescent properties of four diverse complexes with a new symmetric benzimidazolic ligand. *Polyhedron* **2008**, *27*, 3529–3536. [[CrossRef](#)]
69. Che, G.B.; Liu, C.B.; Liu, B.; Wang, Q.W.; Xu, Z.L. Syntheses, structures and photoluminescence of a series of metal-organic complexes with 1,3,5-benzenetricarboxylate and pyrazino[2,3-*f*][1,10]-phenanthroline ligands. *Cryst. Eng. Commun.* **2008**, *10*, 184–191. [[CrossRef](#)]



© 2017 by the authors. Licensee MDPI, Basel, Switzerland. This article is an open access article distributed under the terms and conditions of the Creative Commons Attribution (CC BY) license (<http://creativecommons.org/licenses/by/4.0/>).